

# Planning and Investment Decisions for a Highway Self-Sustained Microgrid System

Longfei Cheng

North China Electric Power University, School of Control and Computer Engineering, Changping District, Beijing, China

Email: [chenglongfei@ncepu.edu.cn](mailto:chenglongfei@ncepu.edu.cn)

**Abstract:** *To address the challenges of highway energy supply in remote areas, renewable energy intermittency, and the limitations of conventional diesel-based power supply, this paper proposes a coordinated source-storage-load planning framework for an off-grid Highway Self-Sustained Microgrid System (HSMS). An optimal sizing model is developed with the objective of minimizing the equivalent annual cost, subject to constraints on power balance, energy storage operation, distributed generation output, and conventional generation unit operation. A case study based on an actual highway section is conducted to verify the proposed method. The results show that, compared with battery-only and hydrogen-only storage schemes, the battery-hydrogen hybrid storage scheme reduces the annual total cost by 2.72% and 6.56%, respectively, while lowering the renewable energy curtailment rate to 0.38% and the outage rate to 0.26%. Hybrid energy storage effectively combines the fast response capability of batteries with the long-duration energy shifting capability of hydrogen storage, thereby enhancing the economic performance, renewable energy utilization, and supply reliability of off-grid highway energy systems. The proposed approach can provide theoretical support for the low-carbon and energy-autonomous development of highway energy infrastructure in off-grid regions.*

**Keywords:** Integration of energy and transportation; Highway Self-Sustained Microgrid System; Optimal sizing; Hybrid energy storage

## 1. Introduction

Transportation emissions rank among the highest across all sectors, and achieving low-carbon development through the intelligent and digital transformation of the transportation industry has become a major trend [1]. Energy underpins transportation operations, while transportation serves as an important carrier for energy consumption [2]. Against this background, the construction of a green and clean Highway Self-Sustained Microgrid System (HSMS) based on the energy-oriented use of transportation infrastructure, thereby promoting the integrated development of the transportation and energy sectors, has attracted growing attention in recent years [3].

The establishment of a flexible, efficient, and intelligent integrated transportation-energy system can provide improved strategies for energy dispatch and management in transportation systems. Based on the concept of integrated development, Wu et al. proposed a system model and technical architecture for the integration of information networks, energy networks, and transportation networks, thereby providing technical support for the implementation of such three-network integration [3]. Yang et al. analyzed three forms of emerging transportation-energy systems from the perspectives of energy dominance, transportation dominance, and balanced energy-transportation development, namely interconnected power grids, electrified transportation, and integrated transportation-energy networks [5]. Although these integrated systems under the three-network convergence framework have broken the traditional barriers between the energy and transportation sectors, substantial research on the coordinated operation of transportation-energy systems under source-load matching conditions remains limited.

Dai et al. analyzed the feasibility of matching highway transportation energy demand with renewable energy supply based on existing classifications of highway energy

consumption [6]. Han et al. proposed a method for assessing the photovoltaic power generation potential of highway slopes, providing a reference for the planning and design of highway photovoltaic projects [7]. Sun et al. developed a novel road energy harvesting system capable of converting the dissipated kinetic energy of moving vehicles into electricity, and case studies demonstrated its feasibility and practicality for near-zero-energy toll stations on highways [8]. Liu et al. integrated wind and solar highway microgrids into the utility grid and proposed an adaptive control strategy for highway microgrid systems, achieving energy management of multiple highway microgrids in the grid-connected mode by regulating the energy flow between the microgrids and the main grid [9]. Teng et al. proposed a multi-source microgrid for zero-waste charging service areas by coordinating waste pyrolysis and gasification facilities with a multi-energy system [10]. Case studies verified that the proposed microgrid can meet the charging demands of electric vehicles and hydrogen-powered vehicles while simultaneously satisfying the waste treatment needs of service areas and surrounding regions.

In summary, most existing studies focus on microgrid systems connected to the main power grid and fail to consider the influence of regional differences in natural resource endowments. To address this gap, this paper considers the uncertainty of regional renewable energy resources, such as wind and solar power, as well as local load characteristics, and proposes a hybrid energy storage planning framework for the HSMS. On the basis of minimizing energy cost, the proposed framework aims to reduce wind and solar curtailment rates while ensuring reliable power supply. Finally, a case study based on an actual highway microgrid system is conducted to validate the effectiveness of the proposed model.

## 2. Architecture of the HSMS

The western region of China is located in off-grid fringe

areas, where abundant wind and solar resources create favorable conditions for the planning, construction, and operation of standalone microgrids. As illustrated in **Figure 1**, the HSMS is composed of renewable energy generation, highway transportation electrical loads, and a hybrid energy storage network, thereby forming a novel transportation-energy system characterized by the coordinated interaction of source, load, and storage.

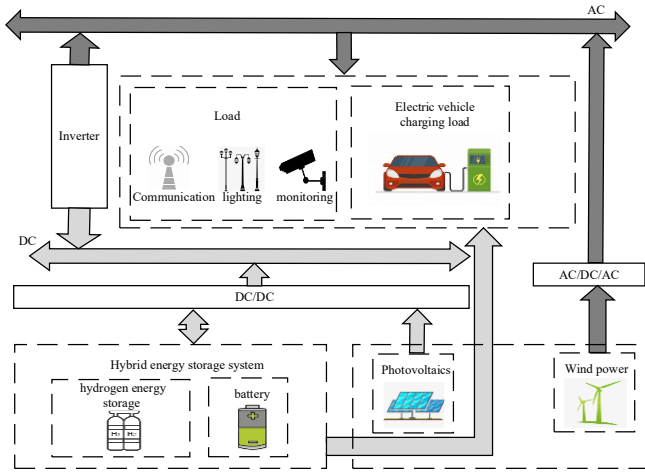


**Figure 1:** Overall HSMS architecture

### 3. System Model

#### 3.1 Distributed Generation Unit Models

The output of a photovoltaic (PV) generation system is mainly affected by factors such as geographical location, solar irradiance, and ambient temperature, and can be expressed as follows:

$$P_{pv} = P_s \frac{G(\rho, m, d, t)}{S_{st}} [1 + \theta_i (T - T_{ref})] \quad (1)$$

Where  $P_{pv}$  is the rated power of the PV panel;  $G(\rho, m, d, t)$  is the hourly average global solar irradiance at the surface of the installation site;  $\rho, m, d, t$  denote the local latitude, month, and hour, respectively;  $S_{st}$  is the standard solar irradiance;  $\theta_i$  is the power temperature coefficient of the PV panel;  $T$  is the actual operating temperature of the PV panel;  $T_{ref}$  is the reference operating temperature of the PV panel.

The output power of a distributed wind power (WT) generation system is mainly determined by the rated power of the wind turbine, the hub height, and the wind speed at the hub height, and can be expressed as follows:

$$P_{wt} = \begin{cases} 0 & S < S_{ci} \\ \frac{S^3 - S_{ci}^3}{S_R^3 - S_{ci}^3} P_R & S_{ci} \leq S < S_R \\ P_R & S_R \leq S < S_{co} \\ 0 & S \geq S_{co} \end{cases} \quad (2)$$

Where  $P_{wt}$  is the actual output power of the wind turbine,  $P_R$  is the rated power of the wind turbine,  $S$  is the actual wind speed at the hub height;  $S_{ci}$ ,  $S_R$ ,  $S_{co}$  are the cut-in wind speed, rated wind speed, and cut-out wind speed of the wind turbine, respectively.

To ensure power supply reliability, this paper uses diesel engines and micro gas turbines as backup generators.

#### 3.2 Energy Storage System Models

To ensure the safe and stable operation of the HSMS system, the battery plays an important role in the overall system. In order to protect battery health, avoid over-discharge, reduce the frequency of deep discharge, and extend battery service life, the state of charge (SOC) of the battery should be maintained within a certain healthy operating range during the discharge process, so that the battery can operate steadily over the long term. The charging and discharging models of the battery are given as follows:

$$SOC(t) = SOC(t-1) + \frac{P_{B, ch} \xi_{ch}}{E_c} \quad (3)$$

$$SOC(t) = SOC(t-1) + \frac{P_{B, dis} \Delta t}{E_c \xi_{dis}} \quad (4)$$

where  $SOC(t)$  and  $SOC(t-1)$  are the state of charge of the battery at time  $t$  and  $t-1$ , respectively;  $\xi_{ch}$  and  $\xi_{dis}$  are the charging efficiency and discharging efficiency of the battery, respectively;  $P_{B, ch}$  and  $P_{B, dis}$  are the charging power and discharging power of the battery, respectively;  $E_c$  is the rated capacity of the battery.

Since the HSMS operates without support from the main power grid and the battery is subject to capacity limitations, excess renewable energy may lead to wind and solar curtailment, while insufficient energy supply may result in power shortages. Therefore, a hydrogen energy storage system is introduced to operate in coordination with the battery system.

The electrolyzer can use electricity to produce high-purity hydrogen through water electrolysis. The simplified electrolyzer model can be expressed as:

$$V_{H_2, ET} = \xi_E P_{FC} = C \eta_f \frac{V_{H_2, FC}}{M_{H_2}} P_{\Omega, \min} \leq P_{\Omega}(t) \leq P_{\Omega, \max} \quad (5)$$

where  $V_{H_2, ET}$  is the volume of hydrogen produced by the electrolyzer;  $\xi_E$  is the electrolysis efficiency of the electrolyzer;  $P_{ET}$  is the input power of the electrolyzer.

The hydrogen storage tank model can be expressed as:

$$E_{H_2}(t) = E_{H_2}(t-1) + \eta_{ch} P_{H_2, ch}(t) - \frac{P_{H_2, dis}(t)}{\eta_{dis}} \quad (6)$$

where  $E_{H_2}(t)$  and  $E_{H_2}(t-1)$  are the storage capacities of the hydrogen tank at time  $t$  and  $t-1$ ; and  $P_{H_2, ch}(t)$  and  $P_{H_2, dis}(t)$  are the hydrogen charging and discharging power of the hydrogen storage tank (HST) at time  $t$ , respectively.

Hydrogen fuel cells generate electricity by consuming hydrogen, and their simplified model can be expressed as:

$$P_{fc} = C \eta_f \frac{V_{H_2, FC}}{M_{H_2}} \quad (7)$$

where  $P_{fc}$  is the output power of the hydrogen fuel cell;  $\eta_f$  is the energy conversion efficiency of the hydrogen fuel cell;  $V_{H_2,FC}$  is the volume of hydrogen consumed by the hydrogen fuel cell;  $M_{H_2}$  is the molar mass of hydrogen;  $C$  is a conversion constant.

### 3.3 Objective Function

In this section, the optimization objective of the HSMS is to minimize the equivalent annual cost of the system. The decision variables are the installed numbers of wind turbines, photovoltaic panels, batteries, hydrogen energy storage units, diesel generators, and micro gas turbines to be planned:

$$C_N = C_{initial} + C_{om} \quad (8)$$

where  $C_{initial}$  is the initial investment cost of the distributed generation units, distributed energy storage units, diesel generators, and micro gas turbines in the system, and  $C_{om}$  is the annual operation and maintenance cost of the distributed generation units, distributed energy storage units, diesel generators, and micro gas turbines.

### 3.4 Constraints

The output constraints of the energy units are as follows:

$$P_{\Omega, \min} \leq P_{\Omega}(t) \leq P_{\Omega, \max} \quad (9)$$

Where  $\Omega$  denotes the set of generation units;  $P_{\Omega, \min}$  and  $P_{\Omega, \max}$  are the minimum and maximum power outputs of each unit, respectively.

The state-of-charge constraint of the battery and the capacity state constraint of the hydrogen storage tank are given as follows.

$$SOC_{\min} \leq SOC(t) \leq SOC_{\max} \quad (10)$$

$$SOH_{\min} \leq SOH(t) \leq SOH_{\max} \quad (11)$$

Where  $SOC_{\min}$  and  $SOC_{\max}$  are the lower and upper limits of the battery state of charge;  $SOH_{\min}$  and  $SOH_{\max}$  are the lower and upper limits of the hydrogen storage tank state of capacity.

The system power balance constraint can be expressed as:

$$P_{wt}^t + P_{pv}^t + P_{dbat}^t + P_{fc}^t + P_{DE}^t + P_{MT}^t = P_{load}^t + P_{cbat}^t + P_{ele}^t \quad (12)$$

where  $P_{dbat}^t$  is the battery charging power at time  $t$ ,  $P_{DE}^t$  is the diesel generator power,  $P_{DE}^t$  is the micro gas turbine output at time  $t$ ,  $P_{cbat}^t$  is the battery discharging power at time  $t$ ,  $P_{load}^t$  is the system load power at time  $t$ ,  $P_{ele}^t$  is the electrolyzer output at time  $t$ .

## 4. Experimental Results and Analysis

### 4.1 Scenario Selection

To be consistent with the assumptions of this study, the Golmud–Lhasa section of the Beijing–Tibet Expressway in China was selected as the case study scenario. The annual average wind speed, solar irradiance, temperature, and

highway load data of this section were taken as the system inputs. The wind and photovoltaic power outputs were calculated using Eqs. (1) and (2), as shown in **Figure 2**, **Figure 3**. The wind power output of the system is mainly concentrated during nighttime, whereas photovoltaic power is generated only during daytime, indicating a strong complementary characteristic between wind and solar energy. The mean output curves shown in the figure were then adopted as representative typical-day profiles for the analysis.

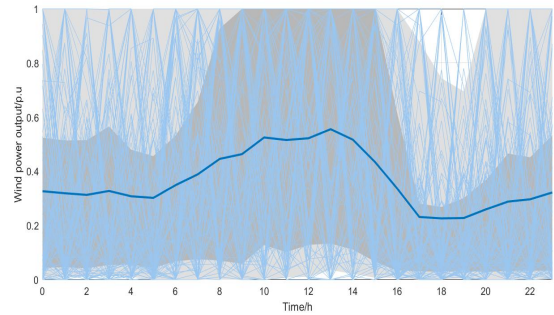


Figure 2: Wind Power Output Profile

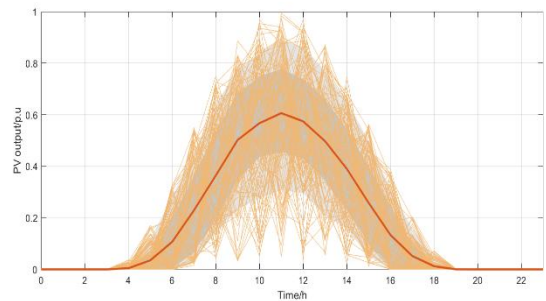


Figure 3: Photovoltaic Power Output Profile

### 4.2 Convergence Analysis of the Algorithm

To validate the proposed scenario settings and evaluate the global search capability and convergence performance of the particle swarm optimization (PSO) algorithm in solving the HSMS planning model, two comparative planning schemes are considered in this section. In the first scheme, only battery storage is considered for power regulation and energy storage; in the second scheme, only a hydrogen-based generation system is considered for power regulation and energy storage. The main equipment parameters of the HSMS planning model are listed in **Table 1**[11].

Table 1: Main Technical and Cost Parameters of Equipment

Equipment	Specification	Investment Cost	Operation and Maintenance Cost
WT	100kW	8500CNY	0.02CNY
PV	2kW	9000CNY	0.008CNY
Battery	12kWh	1000CNY	0.08CNY
Electrolyzer	1kW	9500CNY	0.03CNY
HST	1kg	1800CNY	0 CNY
Fuel cell	1kW	8700CNY	0.05CNY
Gas turbine	30kW	1300CNY	0.045CNY

Based on the planning configurations described above, 50 simulation experiments were conducted for each of the three proposed planning schemes. To reduce the influence of random factors, the population size was set to 60 and the maximum number of iterations was set to 400 for all scenarios. For each scenario, the optimal value and the average value were obtained from 50 independent simulation

runs. The simulation results of the particle swarm optimization algorithm for the three planning schemes are presented in **Table 2** (annual total cost, 10000CNY)

**Table 2:** Simulation Results of the Three Planning Schemes

Scheme	Optimal Value	Mean Value	Variance
Battery storage	955.89	954.97	1.6
HST	988.14	988.03	2.1
Battery&HST	925.89	926.02	2.8

As shown in **Table 2**, the variances of the particle swarm optimization algorithm for the three planning schemes are 1.6, 2.1, and 2.8, respectively. Since the system complexity of the three planning schemes increases progressively, the variance of the hybrid energy storage scheme is slightly higher than

that of the other two schemes. Overall, however, the simulation results of all three planning schemes remain within a relatively small fluctuation range. These results indicate that the particle swarm optimization algorithm exhibits good convergence characteristics and strong global search capability in solving the power capacity planning model of the HSMS.

### 4.3 Experimental Results

Based on the equipment parameters described above, the optimal capacity allocation results for the three HSMS planning schemes obtained using the particle swarm optimization algorithm are presented in **Table 3**.

**Table 3:** Experimental results of each method

Scheme	WT/kW	PV/kW	Electrolyzer/kW	Battery/kWh	HST/kg	Fuel cell/kW	Gas turbine/kW
Battery	300	381	0	623	0	0	167
HST	38	370	45	0	77	21	108
Battery & HST	27	393	19	400	50	6	98

By comparing the power source configuration results of the three planning schemes, it can be seen that, relative to the two comparative schemes employing only a single energy storage mode, the hybrid energy storage scheme adopted in this study, which integrates battery storage and a hydrogen-based power generation system, significantly reduces the capacity allocation required for the storage system under a single-storage configuration. As a result, the total system cost is reduced by 2.72% and 6.56%, respectively, compared with the first two schemes.

**Table 4:** Experimental results of each method

Scheme	Wind/Solar Curtailment Rate	Power Outage Rate
Battery	1.68%	6.21%
HST	2.3%	2.32%
Battery & HST	0.38%	0.26%

As shown in **Table 4**, the hybrid energy storage system absorbs surplus electricity through a small number of electrolyzers and stores it in hydrogen storage tanks, while during peak-load periods, the hydrogen fuel cells discharge to compensate for the power deficit. This configuration substantially reduces the required battery capacity. During system operation, it ensures both renewable energy utilization and power supply reliability, reduces penalty costs, thereby yielding the lowest total system cost among all schemes. In addition, the hybrid energy storage mode provides better temporal shifting of electrical energy, which reduces the required capacity of gas turbines. Meanwhile, part of the more expensive hydrogen storage system is replaced by batteries, further lowering the investment cost of the system and making this scheme the planning configuration with the best overall performance.

## 5. Conclusion

To effectively address the clean energy demand of highway transportation infrastructure, this paper focuses on the HSMS as the research object. For off-grid areas, a planning and investment framework for an HSMS considering the uncertainty of wind and photovoltaic power output is

developed. Meanwhile, a hydrogen-based power generation system is introduced, enabling flexible capacity allocation of each device according to the charging and discharging power of the energy storage system. This has the potential to reduce the required capacities of distributed energy resources and battery storage, thereby improving the overall economic performance of the system.

## References

- [1] HE Z, XIANG Y, LIAO K, et al. Demand, form and key technologies of integrated development of energy-transport-information networks. *Automation of Electric Power Systems*, 2021, 45(16): 73-86.
- [2] SHI T, XU C, DONG W, et al. Research on energy management of hydrogen electric coupling system based on deep reinforcement learning[J]. *Energy*, 2023, 282: 128174.
- [3] JIA L, SHI R, JI L, et al. Research report on integrated development strategy of rail and road transportation and energy: Road [R]. Beijing: Strategic consulting report of Chinese Academy of Engineering, 2022.
- [4] WU T, LIU S, NI M et al. Model design and structure research for integration system of energy, information and transportation networks based on ANP-fuzzy comprehensive evaluation[J]. *Global Energy Interconnection*, 2018, 1(2): 137-144.
- [5] YANG Y, WU P, CHENG P, et al. Development strategy for energy system of land transport in China[J]. *Strategic Study of CAE*, 2022, 24(03):153-162.
- [6] DAI L, ZHANG C, HUANG Y, et al. Feasibility Analysis of Supply-Demand Matching between Highway Operational Energy Consumption and Renewable Energy Integration: A Case Study of Panzhihua-Dali Highway within Sichuan Province[C]//2022 IEEE/IAS Industrial and Commercial Power System Asia (I&CPS Asia). IEEE, 2022: 1989-1993.
- [7] HAN Z, ZHOU W, SHA A, et al. Assessing the Photovoltaic Power Generation Potential of Highway Slopes[J]. *Sustainability*, 2023, 15(16):12159.

- [8] SUN M, WANG W, ZHENG P, et al. A novel road energy harvesting system based on a spatial double V-shaped mechanism for near-zero-energy toll stations on expressways[J]. *Sensors and Actuators A: Physical*, 2021, 323: 112648.
- [9] LIU Y, WANG Y, LI Y, et al. Multi-agent based optimal scheduling and trading for multi-microgrids integrated with urban transportation networks[J]. *IEEE Transactions on Power Systems*, 2020, 36(3): 2197-2210.
- [10] TENG Y, YAN J, HUI Q, et al. Optimization operation model of “zero-waste” electricity-hydrogen charging service area multi-energy microgrid[J]. *Proceedings of the CSEE*, 2021, 41(06): 2074-2088.
- [11] ZHOU Yihuan, XIA Zhiping, LIU Xingbo, et al. Online energy management optimization of hybrid energy storage microgrid with reversible solid oxide cell: A model-based study[J]. *Journal of Cleaner Production*, 2023, 423: 138663.